condensed matter

MDPI

Review

Orbital Symmetry and Orbital Excitations in High-T_c Superconductors

Andrzej M. Oleś [1,2,*], Krzysztof Wohlfeld [3] and Giniyat Khaliullin [1]

1 Max Planck Institute for Solid State Research, Heisenbergstrasse 1, D-70569 Stuttgart, Germany; Giniyat.Khaliullin@fkf.mpg.de
2 Marian Smoluchowski Institute of Physics, Jagiellonian University, Prof. S. Łojasiewicza 11, PL-30348 Kraków, Poland
3 Institute of Theoretical Physics, Faculty of Physics, University of Warsaw, Pasteura 5, PL-02093 Warsaw, Poland; Krzysztof.Wohlfeld@fuw.edu.pl
* Correspondence: a.m.oles@fkf.mpg.de

Received: 12 March 2019; Accepted: 2 May 2019; Published: 6 May 2019

Abstract: We discuss a few possibilities of high-T_c superconductivity with more than one orbital symmetry contributing to the pairing. First, we show that the high energies of orbital excitations in various cuprates suggest a simplified model with a single orbital of $x^2 - y^2$ symmetry doped by holes. Next, several routes towards involving both e_g orbital symmetries for doped holes are discussed: (i) some give superconductivity in a CuO_2 monolayer on Bi2212 superconductors, $Sr_2CuO_{4-\delta}$, $Ba_2CuO_{4-\delta}$, while (ii) others as nickelate heterostructures or $Eu_{2-x}Sr_xNiO_4$, could in principle realize it as well. At low electron filling of Ru ions, spin-orbital entangled states of t_{2g} symmetry contribute in Sr_2RuO_4. Finally, electrons with both t_{2g} and e_g orbital symmetries contribute to the superconducting properties and nematicity of Fe-based superconductors, pnictides or FeSe. Some of them provide examples of orbital-selective Cooper pairing.

Keywords: high-T_c superconductivity; orbital symmetry; orbital excitation; charge-transfer insulator; Fermi surface; spin-orbit coupling; spin-orbital entanglement; electron-phonon; Cooper pairing

1. Introduction: Towards Superconductivity with Orbital Degrees of Freedom

Significance of the discovery of high-T_c superconductivity by Bednorz and Muller [1] for recent progress in the quantum many-body theory cannot be overestimated—it triggered a huge amount of innovative research on quantum materials and unconventional superconductors, both in the experiment and in the theory. In spite of reaching a qualitative understanding of the nature of the superconducting (SC) state in different transition metal compounds, several open problems remain. Some are related to cuprates, as the astonishing complexity of the phase diagram and the physical origin of the temperature T^* observed well above T_c itself [2–6]; others are more general and include questions about the origin of pairing [7–11], optimal conditions for the onset of the SC state [12–15], variation under pressure [16], and the actual orbital symmetry at the Fermi surface [17].

In this short review we concentrate on the last question. After the discovery of high-T_c superconductivity in cuprates it was believed that lifting of degeneracy of e_g orbitals was important to obtain the SC state with a high value of T_c [18–20]. Indeed, typically in cuprates degeneracy is quite lifted and relevance of Jahn-Teller effect is controversial. It is under discussion whether the effective model for cuprates has nondegenerate orbitals and may be represented by extended Hubbard model with on-site Coulomb and further neighbor hopping [21]. Yet, it is derived for the case of large splitting of e_g orbitals, while orbital degrees of freedom might play an important role in the SC instability and the multiorbital Hubbard model is a standard model for all high-T_c superconductors in general, where the dome of T_c occurs by driving the chemical potential in the proximity of a Lifshitz transition [22].

We shall not address here the role played by electron-phonon coupling which is expected to contribute in cuprates and is a driving force of recently discovered superconductivity in H_3S [23,24]. In particular, since the degenerate orbital degrees of freedom necessarily come along with strong Jahn-Teller coupling [25,26], the electron-phonon coupling seems to be essential for SC instabilities in all systems with orbital degeneracy. Nevertheless, to make this review more focused, we shall limit ourselves to the consequences of the orbital degeneracy for the models containing solely electronic degrees of freedom—thus leaving the interplay of the electron-phonon coupling and the orbital degeneracy in the high-T_c superconductors for another work.

The outline of this paper is as follows. One early idea in the theory of cuprate superconductivity was that orbital excitations could contribute to the pairing mechanism, as discussed also in Section 2.1, but this was not supported by more recent developments. A usual situation is that the pairing occurs for holes in a single molecular orbital of $x^2 - y^2$ symmetry, see Section 2.2. But certainly an interesting question is whether allowing for the presence of holes in both e_g orbitals would not lead to enhanced SC instabilities. This idea has its roots in the Jahn-Teller physics in cuprates [25,26], as well as in the observation that the propagation of a hole in a Mott (or charge-transfer) insulator is much richer when both e_g orbitals can participate [27]. Partial filling of both e_g orbitals could be realized in the highly overdoped CuO_2 monolayer grown on $Bi_2Sr_2CaCu_2O_{8+\delta}$ (Bi2212) [28,29]. We remark that the symmetry of the SC phase in Bi2212 has been extensively discussed in the literature (see, e.g., [30–35]).

Furthermore, we emphasize that two-dimensional (2D) systems are special, and possible SC instability was predicted for a layered geometry of NiO_2 planes in $LaNiO_3/LaMO_3$ superlattices [36]. We follow this idea and discuss briefly remarkable similarity between overdoped cuprates and nickelates in Sections 3.1 and 3.2. Furthermore, superconductivity occurs also in metallic systems with t_{2g} degrees of freedom, i.e., in planar ruthenate Sr_2RuO_4 (Section 3.3) and in Fe-based superconductors (Section 3.4). In the latter systems orbital fluctuations are expected to contribute [8,37]. The former systems are of particular interest as there spin-orbit interaction entangles spin-orbital degrees of freedom and the orbital states become mixed [38]. A planar iridate Sr_2IrO_4 with an even stronger spin-orbit coupling shows much of the cuprate phenomenology [39], but no superconductivity was reported so far. This review is summarized in Section 4.

2. The Role of Orbitals in Superconducting Cuprates

2.1. Earlier Theoretical Proposals

Following the idea of Jahn-Teller physics in cuprates [25,26], a question arises how many orbital symmetries should be included in a minimal realistic model for cuprates. Already in the early years of high-T_c, the idea of going beyond the single band picture by including O($2p$) orbitals in the three-band model has emerged [40–42]. Whether or not the oxygen orbitals could be fully integrated out is still not fully resolved [43–45]. Leaving this issue open, we shall present here an overview of the role played by the copper orbital degrees of freedom.

It has been discussed early on that multiple orbitals contribute to the physical properties of $YBa_2Cu_3O_{7-x}$ [46–48] and $La_{2-x}Sr_xCuO_4$ [49,50]. The coupling to the lattice was employed as sensitive to the orbital content of wave-functions — multiorbital components were deduced from uniaxial and hydrostatic pressure effects on the value of T_c [51], and from the effect of rhombic distortion on the polarized x-ray absorption spectra in high-T_c superconductors [52].

Further research on stripes and electron-lattice interactions suggested the presence of pseudo-Jahn-Teller effect in cuprates [53–56]. These phenomena follow in a natural way from orbital pseudo-degeneracy [57], and these ideas were further developed in [58–62]. Support for the relevance of electron-phonon interaction comes from the observation of the isotope effect on the pseudogap temperature T^* [63], from strong renormalization of certain phonons by doped holes [64], and from recently observed phonon anomalies in charge density wave states in cuprates [65,66].

Already shortly after the discovery of high-T_c cuprates, it was suggested by Weber [67] that an orbital excitation could be responsible for the pairing. In a typical copper oxide the nearest neighbor Coulomb interaction between holes in the oxygen p orbitals and the copper $3z^2 - r^2$ orbital is substantially smaller than between holes in the oxygen p orbitals and the Cu $x^2 - y^2$ orbital — such an aspherical Coulomb interaction is estimated to be of the order of 0.3-0.5 eV in the cuprates [67]. Consequently, an excitonic pairing mechanism was proposed: two oxygen holes can gain energy provided that the first one excites the Cu d hole from the $x^2 - y^2$ to the $3z^2 - r^2$ orbital and the second one follows, forming a pair. This mechanism was later further improved by Jarrell, Cox, and others [68,69] by including the superexchange processes between the nearest neighbor oxygen p orbitals and both Cu e_g orbitals. This latter mechanism was estimated to roughly triple the strength of the coupling between the orbital exciton and the holes on oxygen.

While the above proposal is appealing, unfortunately it is not very realistic: the crucial role played by the copper spins is completely neglected and it is implicitly assumed that the doped holes go to the π-bonding oxygen orbitals. A more realistic two-orbital e_g model was proposed in [27], and the onset of superconductivity in the various versions of the two-orbital Hubbard models was studied in more detail, e.g., in [70–73]. Nevertheless, in order to verify whether these models could be relevant to the cuprate superconductivity, it is crucial to include the size of the crystal-field splitting between the Cu $3z^2 - r^2$ and $x^2 - y^2$ orbitals—as discussed in the next subsection.

2.2. Orbital Excitations in Cuprates

In a 'typical' high-T_c cuprate, the CuO_6 octahedra are elongated along the c axis due to apical oxygen displacements, and the degeneracy of e_g orbitals is lifted. It has been established that both electron-doped and hole-doped copper oxides are strongly correlated electron systems in the vicinity of the metal to charge-transfer insulator transition [74]. One also finds large splitting of the copper $3d$ states and only a single Cu($3d$)–O($2p$) hybridized band crosses the Fermi surface in doped systems. This band has the $x^2 - y^2$ symmetry and becomes half-filled in the undoped charge-transfer insulator La_2CuO_4. The superexchange stabilizes then antiferromagnetic (AF) order [75] in this and other compounds of the cuprate family [2,3]. Doping generates a Fermi surface originating from a single band made of oxygen $2p$ and copper $3d$ states, for small hole doping $x < 0.3$, as discussed by Zhang and Rice [76], see Figure 1. In this regime d-wave SC phase is found, and a high value of T_c is obtained when the orbital splitting is large [18–20].

Interestingly, it has taken almost 20 years both for the experiment and the theory to unequivocally agree on the energies of the (local) orbital excitations on the copper ion of the undoped cuprates ("$d - d$ excitations" [27]). It has long been believed that, while the ground state orbital is of $x^2 - y^2$ character, the energy of the $3z^2 - r^2$ orbital excitation is rather low, for instance of the order of $\sim$0.4 eV—as suggested by the optical and resonant inelastic x-ray scattering (RIXS) measurements of La_2CuO_4 [77,78] as well as by optical absorption for $Sr_2CuO_2Cl_2$ [77]. The latter result is particularly striking, for the most recent understanding (see Table 1 and discussion below) is that the $3z^2 - r^2$ orbital excitation is not even the lowest lying orbital excitation in $Sr_2CuO_2Cl_2$. Though, even earlier the above result was challenged by Lorenzana and Sawatzky [79], suggesting a different interpretation of the optical absorption spectra, in which the 0.4 eV feature was assigned to the magnetic excitations. Finally, these results did not agree with the theoretical estimates giving about 0.9 eV energy for such an orbital excitation, according to the density-functional theory [20], or with the X-ray absorption spectroscopy results showing a very weak $3z^2 - r^2$ character in the ground state of the hole-doped cuprates [50].

The recent years have, however, lead to substantial advancements both in the resolution of the RIXS experiments of the cuprates [80] as well as *ab-initio* quantum chemistry calculations [81], and allowed for obtaining the results for cuprates [81,82] in remarkable agreement between the theory and experiment, as presented in Table 1. We emphasize that nowhere one can find the above-mentioned low values of the orbital excitation energies, for all excitations have their energies substantially

above 1 eV. Finally, it is only in La_2CuO_4 that the lowest energy orbital excitation has a $3z^2 - r^2$ character; otherwise this excitation has the *highest* energy. In general, a more detailed study of various other copper oxides, with/without apical ligands, suggests that the energy of the $3z^2 - r^2$ orbital correlates with the out-of-plane Cu-ligand distance h, although this relation is rather complex (cf. Figure 1 of [81]).

Table 1. The energies of orbital excitations in various undoped cuprates, as obtained form the RIXS experiment [82] (quantum-chemistry calculations [81]). Note that a classical magnetic exchange energy $2J \simeq 0.26$ eV is subtracted from all given energy values. Table adopted from [81].

Cu(3*d*) Orbital	La_2CuO_4	$Sr_2CuO_2Cl_2$	$CaCuO_2$
$3z^2 - r^2$	1.44 (1.37)	1.71 (1.75)	2.39 (2.38)
xy	1.54 (1.43)	1.24 (1.16)	1.38 (1.36)
xz/yz	1.86 (1.78)	1.58 (1.69)	1.69 (2.02)

This situation is somewhat more subtle in doped cuprates. Again, in the early years of high-T_c research, it was expected that the occupancy of the low-lying orbital $3z^2 - r^2$ would increase upon doping [47,83–85]. However, as just discussed, in 'most' of the cuprates this orbital turns out to be the highest lying one in the undoped crystals, such a scenario now seems to be no longer relevant. Instead, (typically) the lowest lying xy orbital either hardens by about 50 meV [86], or softens by 150 meV [87] with doping, depending on the compound. Moreover, in both cases the lowest lying $d - d$ excitation has an energy by $\sim$1.5 eV higher than the ground state orbital even in SC samples [88], in agreement with Table 1.

The above discussion shows that the orbital excitations in the cuprates have relatively high energies, suggesting that the electrons close to the Fermi surface are clearly of a single 3*d*-band character. Surprisingly, however, some important signatures of the so-called *orbital physics* [89–102] are visible there: clear experimental signatures of the collective orbital excitation, the orbiton, have been observed in the quasi-one-dimensional (quasi-1D) copper oxides [97,98]. To a large extent this turned out to be possible due to the strong crystal-field splitting of the orbital excitations [99,100]. The search for similar phenomena in the quasi-2D (i.e., high-T_c) cuprates is ongoing [103].

3. Superconductivity with Orbital Degrees of Freedom

3.1. Beyond the Cuprates with the Pairing in a Single $x^2 - y^2$ Orbital

A way to enhance the value of T_c in compounds isostructural with La_2CuO_4 was found by Uchida et al. [104]: higher hole doping in CuO_2 planes is realized by replacing La ions by Sr ions in $Sr_2CuO_{4-\delta}$. The SC transition temperature $T_c = 95$ K is then almost doubled for the hole doping $x \simeq 0.8$, see Figure 1. In this regime another nodeless SC phase arises, and the symmetry in the orbital space is partly restored. In fact, also the band of $3z^2 - r^2$ symmetry is partly filled, and the pairing occurs jointly for the B_{1g} and A_{1g} channels in $Sr_2CuO_{4-\delta}$ and also in $Ba_2CuO_{4-\delta}$ [105]. This possibility was discussed a decade ago [106], and was realized, *inter alia*, in a recently discovered superconductor with $T_c > 70$ K [107]. The CuO_6 octahedra are compressed here and $3z^2 - r^2$ orbitals contribute at the Fermi surface. The pairing strength is large relative to a similar calculation for an optimally doped Hubbard model. The theory predicts that the pairing strength depends on the shape of the Fermi surface [105], see the right inset of Figure 1, with nearly square shapes of both electron and hole bands responsible for the enhanced pairing. These results seem to challenge an early view that T_c is optimized when a single band with $x^2 - y^2$ symmetry crosses the Fermi surface [18–20], see also Section 2.

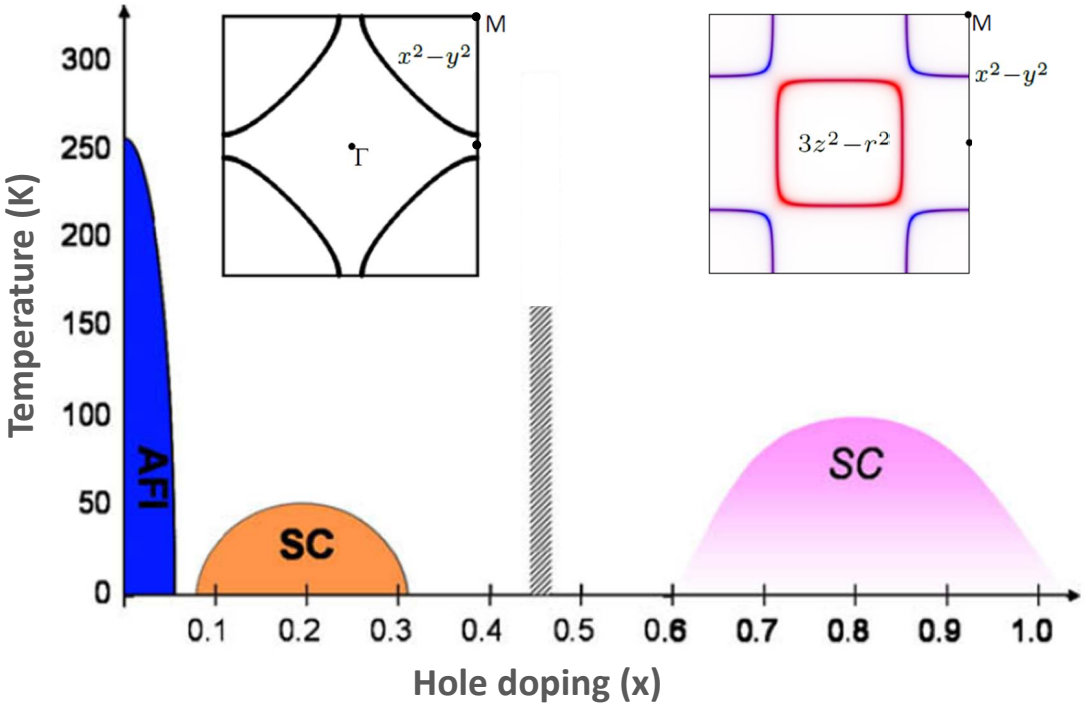

Figure 1. Schematic phase diagram for cuprates as a function of hole doping x, showing the route from the single-band SC phase with holes in x^2-y^2-type molecular orbitals, realized in bulk cuprates (left), to the two-orbital nodeless SC phase in the hole-rich CuO_2/Bi2212 monolayer (right). The insets show the corresponding Fermi surface for one-orbital (left) and two-orbital $\{x^2-y^2, 3z^2-r^2\}$ (right) SC phase. Image is reproduced from [106]; right inset for the hole-rich CuO_2 monolayer is reproduced from [105].

Another way of increasing the hole density in Cu(3*d*) orbitals was realized for a CuO_2 monolayer grown on Bi2212 cuprate [28]. Here the CuO_2 monolayer is heavily overdoped by charge transfer at the interface and has a short bond between Cu and the apical O in the substrate. A minimal two-orbital model predicts indeed a nodeless high-T_c SC state with $s^{\pm}$ pairing [29], arising from the spin-orbital exchange a'la Kugel-Khomskii model [89].

3.2. Nickelates

One expects that another route to achieve higher hole doping in Cu(3*d*) orbitals is realized in Ni oxides, and indeed the Fermi surface very similar to that for the overdoped cuprates was observed in $Eu_{2-x}Sr_xNiO_4$ [108]. This Fermi surface is also similar to the one found for $LaNiO_3/LaAlO_3$ heterostructure, where both e_g symmetries contribute to the band structure obtained in local density approximation (LDA) [109], see Figure 2. Although it was argued that the $3z^2-r^2$ symmetry would be eliminated by electron correlations, both bands were observed in the experiment [108].

The theoretical study of the electronic structure for the $LaNiO_3/LaAlO_3$ heterostructure suggests that *orbital engineering* using heterostructuring is in principle possible. The electronic structure obtained with LDA for the heterostructure without strain, see Figure 2a, has the Fermi surface at $k_z = 0$ very similar to that of the overdoped CuO_2 monolayer, see Figure 2b and the right inset of Figure 1. Hence, the theory predicts a SC heterostructure, if this system could be synthesized in the future. So far, widely tunable orbital configurations were indeed realized by in strongly correlated systems: $LaTiO_3/LaNiO_3/LaAlO_3$ heterostructure [110], and nickelate superlattices [111,112].

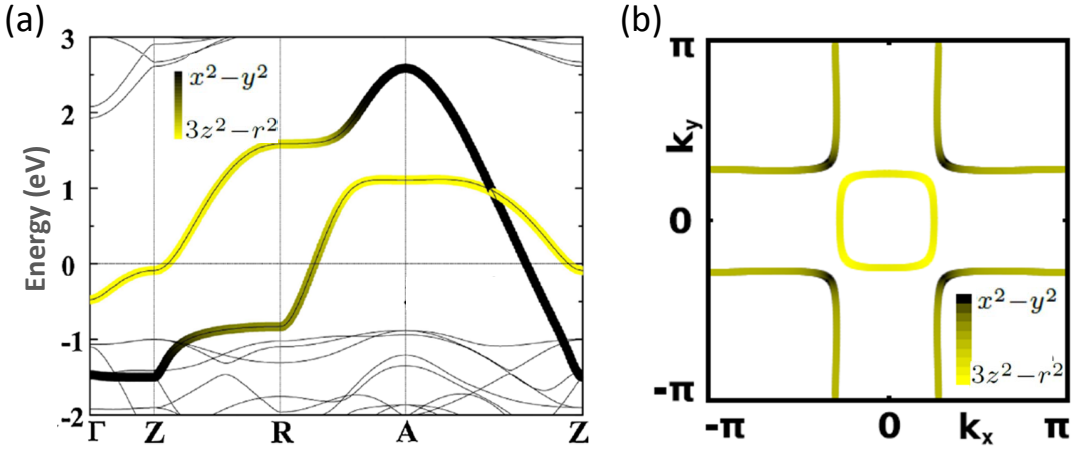

Figure 2. Electronic structure for the $LaNiO_3/LaAlO_3$ heterostructure without strain obtained in the LDA: (**a**) bands of e_g symmetry (black to yellow shading for orbital character), and (**b**) corresponding cross section of the Fermi surface with the $k_z = 0$ plane. Images are reproduced from [109].

Also in other square-planar nickelate, $Pr_4Ni_3O_8$, both e_g orbitals contribute to the Fermi surface [113]. X-ray absorption shows that low-spin configuration with $x^2 - y^2$ character of the hole states is realized there [114], making these states remarkably similar to those in hole-doped cuprates. Hence, also these compounds may be considered as promising candidates for unconventional superconductivity. Recently, a family of Ni-based compounds, which contain $[Ni_2M_2O]^{2-}$ (M-chalcogen) layers with an antiperovskite structure constructed by mixed-anion Ni complexes, has been suggested as possible high-T_c superconductors [115]. Here again both e_g symmetries should contribute, and one expects strong competition between s-wave and d-wave pairing symmetries.

More complicated situations are also possible, and we mention here KNi_2S_2 as an example of a Ni-based superconductor with three different orbital symmetries contributing at the Fermi surface and a small value of $T_c = 0.46$ K [116]. The electronic structure is described by the multiorbital Hubbard model and this system has certain similarity to iron-based superconductors discussed in Section 3.4.

3.3. Superconducting Ruthenate Sr_2RuO_4

The SC state of strontium ruthenate Sr_2RuO_4 was discovered in 1994 by Maeno and his collaborators after they had succeeded in synthesizing high-quality samples of the material [117]. It was soon realized that different orbital symmetries contribute to the SC state in this unique ruthenium oxide [118]. The value of $T_c = 1.5$ K is not particularly high, but the ruthenate structure suggests a possible relationship to the high-T_c cuprate superconductors. Yet, in spite of their structural similarity, doped La_2CuO_4 and Sr_2RuO_4 are quite different [119].

In conventional superconductors, in high-T_c copper oxides, and in Fe pnictides, the Cooper pairs have even parity. In contrast, Sr_2RuO_4 is the candidate for odd parity superconductivity [15]. However, the pairing symmetry in this material is not yet fully established (see, e.g., [120,121]). Ruthenates have active t_{2g} orbital degrees of freedom [122,123], with degenerate yz and zx orbital states. An additional complication in the theory is the presence of a sizeable spin-orbit coupling ($\zeta \sim 90$ meV at the Γ point), which is much smaller than full bandwidth of ∼3 eV but nonetheless leads to important consequences by mixing the low-energy t_{2g} spin-orbital states. As a result, the Fermi surface, consisting of three $\{\alpha, \beta, \gamma\}$ bands [124], changes qualitatively, see Figure 3a. In particular, the crossing points (accidental degeneracies) between the electronic β and γ bands vanish and the Fermi surface for both $\{\beta, \gamma\}$ bands becomes more circular [38], while there is no phase space for mixing of hole-like α band.

For further discussion we focus on the representative β band; the mixing of t_{2g} orbital states remains similar for the other bands. The most important consequence of finite spin-orbit coupling

ζ is momentum-dependent spin-orbital entanglement [38] of the eigenstates near the Fermi surface. It is illustrated in Figure 3b for the β band and three representative values of momentum k_z. Going along the Fermi surface for a fixed value of k_z, one observes that not only the orbital character changes, but also both components of $s = 1/2$ spin mix. The latter mixing of spin components is somewhat weaker for large value of $k_z = 3\pi/4$. This mixing plays an important role and the challenging theoretical problem is to include orbital fluctuations in the theory of superconductivity in Sr_2RuO_4.

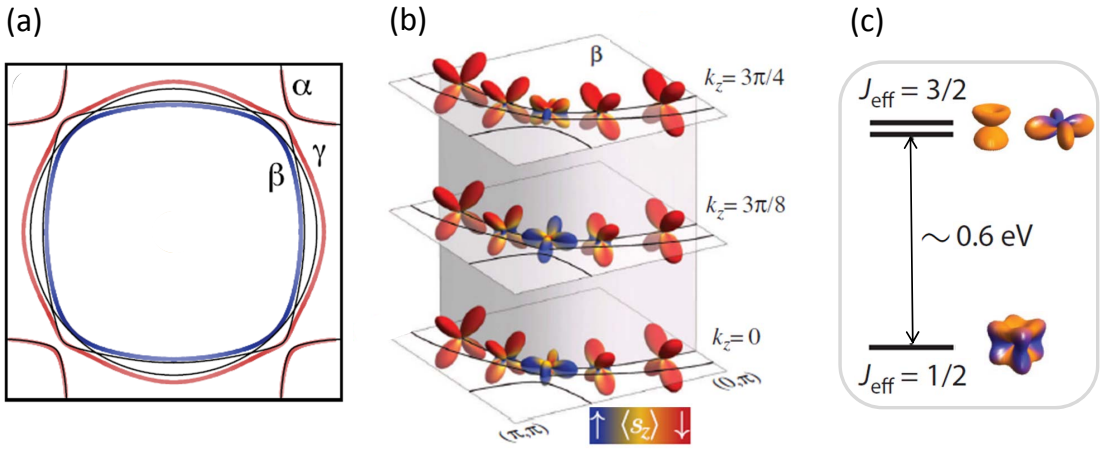

Figure 3. (**a**) and (**b**): Spin-orbital entanglement in Sr_2RuO_4 ruthenate: (**a**) Fermi surface for bands $\{\alpha, \beta, \gamma\}$ at $k_z = 0$ calculated without (thin black) and with (thick, color-coded) spin-orbit $\langle \vec{l} \cdot \vec{s} \rangle$ coupling, and (**b**) momentum-dependent Ru(4*d*) orbital projection of the wave function for the β band at selected momentum locations along the 3D Fermi surface. The orbital color represents the momentum-dependent spin $\langle s^z \rangle$ expectation value; blue/red correspond to spin $\uparrow/\downarrow$ for one state of the Kramers-degenerate pair, see the color scale at bottom right. The strongly mixed colors indicate momentum-dependent spin-orbital entanglement. Images (**a**) and (**b**) are reproduced from [38]. (**c**) Orbital excitations in Sr_2IrO_4 between the entangled spin-orbital ground state (with $J_{\text{eff}} = 1/2$) and the excited doublet (with $J_{\text{eff}} = 3/2$), with the energy much lower than in cuprates (cf. Table 1).

When spin-orbit coupling is large enough, it can unify the spin and orbital subspaces locally, forming the effective pseudospin $J_{\text{eff}} = 1/2$ states that dominate low energy physics [93,125,126]. This case is particulary relevant for iridium oxides, and indeed, a perovskite compound Sr_2IrO_4 was found to host pseudospin $J_{\text{eff}} = 1/2$ antiferromagnetism [127–129], with quasi-2D magnon excitations similar to those of spin $S = 1/2$ in cuprates. It was recently found that spin-orbit entangled magnetism in iridates and ruthenates is strongly influenced by electron-lattice coupling, via pseudo-Jahn-Teller effect [130]. The remarkable analogy between layered iridates and cuprates holds also upon doping—single band Fermi surface, (pseudo)gap, and Fermi arcs have been detected [131]. However, a long-range coherent superconductivity has not been yet found in iridates. Whether this is related to the fact that spin-orbital excitation energies 0.6 eV [129] in iridates, see Figure 3c, are much lower than in cuprates, or to the Mott insulating nature of iridates, in contrast to charge-transfer insulating cuprates, remains an open question. For detailed discussion the similarities and differences between iridates and cuprates, we refer to the recent review article [39].

3.4. Iron-Based Superconductors

Similar to cuprates, the Fe-based superconductors have 2D lattices of 3*d* transition metal ions as building blocks. However, while oxygen ions lie in the same planes as Cu ions in La_2CuO_4, ions of As, P, or Se lie above or below the Fe plane, in positions close to tetrahedral. For this reason, the out-of-plane As orbitals hybridize well with t_{2g} orbitals of Fe ions. In addition, there is a substantial

overlap between the 3*d* orbitals [7–11,132–134]. Under these circumstances, the minimal models for pnictide superconductors contain at least two [135] or three [136] t_{2g} orbitals per Fe atom.

In contrast to undoped cuprates, parent compounds of Fe-based superconductors are metallic [7], and the pairings of different symmetry compete in a two-band model [11,137–139]. The coexistence of hole-like and electron-like bands at the Fermi surface is quite generic [7,8,133]. Then Lifshitz transitions can develop for increasing external magnetic field. Such transitions were indeed found in a two-band model with intra-band pairing [140] and could explain the experimental observations in FeSe and Co-doped $BaFe_2As_2$ compounds. The competition between different pairing symmetries in KFe_2As_2 causes a change of symmetry at the critical pressure, from *d*-wave to s_{++}-wave symmetry [141].

Before discussing the nature of pairing, it is interesting to look at the strong coupling model for pnictides, including magnetic frustration [142]. A spin-orbital model for interacting Fe ions in intermediate $S = 1$ spin states was derived [143] in the regime of strong electron correlations. It highlights Hund's exchange for electron correlations, recently observed experimentally [144]. Magnetic and orbital instabilities are here far richer than in cuprates, and one finds the experimentally observed spin-stripe state which could be accompanied by three different types of orbital order. This is another manifestation of substantial magnetic frustration of the superexchange [142] which may partly explain why magnetic instabilities are sometimes absent, e.g., in FeSe and LiFeAs.

The spin-orbital model [143], however, does not contain biquadratic exchange which was found to be crucial in magnetism of Fe-based superconductors [145–148]. This coupling may originate from spin-state fluctuations [149] typical for Fe-ions in systems with strong $p - d$ covalency. While large biquadratic exchange is quite unique and essential for the description of magnetic and nematic instabilities, its implications for SC instabilities belong to open problems in the field. Indeed, the SC phase in iron-based materials occurs in the vicinity of the two above instabilities: Not only one has the usual magnetic phases [150], but also the nematic order may occur [97,151,152]. A detailed study shows that the Fermi surface of FeSe undergoes a spontaneous distortion from fourfold-symmetric to twofold-symmetric elliptical pockets, and next SC phase emerges from the nematic electronic phase.

The theory of Cooper pairing in Fe-based superconductors is rather involved and still far from complete [8,9,153]. The role played by orbital and spin fluctuations belongs to challenging open problems in the theory. It was found that the orbital fluctuations may give rise to the strong pairing interaction due to the cooperation of Coulomb and electron-phonon interactions [154,155]. The theory explains also the famous empirical relation between T_c and the As-Fe-As bond angle [156].

Altogether, the pairing in iron-based superconductors involves all the five Fe(3*d*) orbitals, and multiple orbital physics gives rise to various novel phenomena like orbital-selective Mott transition, nematicity, and orbital fluctuations that may support the SC phase. Recent theory treating spin and orbital fluctuations on equal footing predicts that, at certain conditions, a spontaneous orbital order sets in first, and then superconductivity follows [157]. The SC gap and low energy excitations in FeSe are dominated by a single *xz* orbital [158] which uncovers the orbital origin of the strongly anisotropic gap in the FeSe superconductor [159–162]. In $LiFe_{1-x}Co_xAs$ spin excitations are orbital selective: low-energy spin excitations are mostly from *xy* orbitals, while high-energy spin excitations arise from the *yz* and *zx* orbitals [163]. Such strongly orbital selective spin excitations in LiFeAs family might play a role in the mechanism of orbital selective Cooper pairing as well.

4. Summary

To conclude, we have presented the current status of the high-T_c superconductivity in the presence of orbital degrees of freedom. As this subject is very broad, in this review we limit the presentation solely to the electronic degrees of freedom, leaving aside a detailed discussion of the role played by their coupling to the lattice. In case of cuprates large hole doping and removing octahedral distortions is necessary to activate the $3z^2 - r^2$ orbitals, and we gave examples of cuprates with two e_g orbitals and higher values of T_c than in $La_{2-x}(Sr,Ba)_xCuO_4$. These orbitals contribute to almost the same Fermi surface, consisting of hole and electron parts, also in doped nickelates. But for nickelates we cannot

present anything more than a theoretical suggestion that the superconducting instabilities could occur as well. Finally, very interesting superconducting states emerge in Sr_2RuO_4 and in iron pnictides, where several t_{2g} symmetries meet at the Fermi surface and participate in the Cooper pairing. Search for other transition metal compounds with SC instabilities continues — for instance, recently AgF_2 was suggested as an excellent analogue to La_2CuO_4 [164], but no superconductivity was observed so far.

> Summarizing, the presence of orbital degrees of freedom makes high-T_c superconductors an even more exciting class of quantum materials where the competing quantum phases are of particular importance for superconductivity in layered compounds [165]. It seems that orbital fluctuations could enhance the superconducting transition temperature T_c, but we emphasize that the role of orbital degrees of freedom in the phenomenon of pairing belongs to open problems in the theory; in particular the interplay between orbital degeneracy and the Jahn-Teller coupling to lattice — the idea that guided Bednorz and Müller in their discovery of high-T_c superconductivity — has to be worked out in a greater detail.

Author Contributions: All authors selected the relevant information, participated in discussions, wrote the manuscript and contributed to the interpretation of the results.

Funding: This research was funded by Narodowe Centrum Nauki (NCN, National Science Centre, Poland) under Projects Nos. 2016/22/E/ST3/00560 and 2016/23/B/ST3/00839.

Acknowledgments: We would like to thank Mona Berciu, Antonio Bianconi, Lucio Braicovich, Jeroen van den Brink, Mario Cuoco, Maria Daghofer, Thomas P. Devereaux, Louis Felix Feiner, Jörg Fink, Andres Greco, Maurits Haverkort, Peter J. Hirschfeld, Peter Horsch, Liviu Hozoi, Huimei Liu, Andrzej Ptok, Roman Puźniak, George A. Sawatzky, Józef Spałek, Hiroyuki Yamase, Alexander N. Yaresko, Jan Zaanen, and Roland Zeyher for many insightful discussions. A. M. Oleś is grateful for the Alexander von Humboldt Foundation Fellowship (Humboldt-Forschungspreis).

Conflicts of Interest: The authors declare no conflict of interest.

References

1. Bednorz, J.G.; Muller, K.A. Possible high-T_c superconductivity in the Ba-La-Cu-O system. *Z. Phys. B* **1986**, *64*, 189–193. [CrossRef]
2. Lee, P.A.; Nagaosa, N.; Wen, X.G. Doping a Mott insulator: Physics of high-temperature superconductivity. *Rev. Mod. Phys.* **2006**, *78*, 17–85. [CrossRef]
3. Ogata, M.; Fukuyama, H. The *t-J* model for the oxide high-T_c superconductors. *Rep. Prog. Phys.* **2008**, *71*, 036501. [CrossRef]
4. Vojta, M. Lattice symmetry breaking in cuprate superconductors: stripes, nematics, and superconductivity. *Adv. Phys.* **2009**, *58*, 699–820. [CrossRef]
5. Bianconi, A.; Poccia, N. Superstripes and complexity in High-Temperature Superconductors. *J. Supercond. Nov. Magn.* **2012**, *25*, 1403–1412. [CrossRef]
6. Keimer, B.; Kivelson, S.A.; Norman, M.R.; Uchida, S.; Zaanen, J. From quantum matter to high-temperature superconductivity in copper oxides. *Nature* **2015**, *518*, 179–186. [CrossRef]
7. Paglione, J.; Greene, R.L. High-Temperature Tuperconductivity in Iron-Based Material. *Nat. Phys.* **2010**, *6*, 645–658. [CrossRef]
8. Hirschfeld, P.J.; Korshunov, M.M.; Mazin, I.I. Gap symmetry and structure of Fe-based superconductors. *Rep. Prog. Phys.* **2011**, *74*, 124508. [CrossRef]
9. Scalapino, D.J. A common thread: The pairing interaction for unconventional superconductors. *Rev. Mod. Phys.* **2012**, *84*, 1383–1417. [CrossRef]
10. Si, Q.; Yu, R.; Abrahams, E. High-temperature superconductivity in iron pnictides and chalcogenides. *Nat. Rev. Mat.* **2016**, *1*, 16017. [CrossRef]
11. Fernandes, R.M.; Chubukov, A.V. Low-energy microscopic models for iron-based superconductors: A review. *Rep. Prog. Phys.* **2017**, *80*, 014503. [CrossRef] [PubMed]
12. Cava, R.J.; Takagi, H.; Zandbergen, H.W.; Krajewski, J.J.; Peck Jr, W.F.; Siegrist, T.; Batlogg, B.; van Dover, R.B.; Felder, R.J.; Mizuhashi, K.; et al. Superconductivity in the quaternary intermetallic compounds $LnNi_2B_2C$. *Nature* **1994**, *367*, 252–253. [CrossRef]

13. Kastner, M.A.; Birgeneau, R.J.; Shirane, G.; Endoh, Y. Magnetic, transport, and optical properties of monolayer copper oxides. *Rev. Mod. Phys.* **1998**, *70*, 897–928. [CrossRef]
14. Imada, M.; Fujimori, A.; Tokura, Y. Metal-insulator transitions. *Rev. Mod. Phys.* **1998**, *70*, 1039–1263. [CrossRef]
15. Mackenzie, A.P.; Maeno, Y. The superconductivity of Sr_2RuO_4 and the physics of spin-triplet pairing. *Rev. Mod. Phys.* **2003**, *75*, 657–712. [CrossRef]
16. Krzton-Maziopa, A.; Svitlyk, V.; Pomjakushina, E.; Puźniak, R.; Conder, K. Superconductivity in alkali metal intercalated iron selenides. *J. Phys. Condens. Mat.* **2016**, *28*, 293002. [CrossRef]
17. Graser, S.; Maier, T.A.; Hirschfeld, P.J.; Scalapino, D.J. Near-degeneracy of several pairing channels in multiorbital models for the Fe pnictides. *New J. Phys.* **2009**, *21*, 025016. [CrossRef]
18. Ohta, Y.; Tohyama, T.; Maekawa S. Apex oxygen and critical temperature in copper oxide superconductors: Universal correlation with the stability of local singlets. *Phys. Rev. B* **1991**, *43*, 2968–2982. [CrossRef]
19. Pavarini, E.; Dasgupta, I.; Saha-Dasgupta, T.; Jepsen, O.; Andersen, O.K. Band-Structure Trend in Hole-Doped Cuprates and Correlation with $T_{c\,\max}$. *Phys. Rev. Lett.* **2014**, *112*, 127002.
20. Sakakibara, H.; Usui, H.; Kuroki, K.; Arita, R.; Aoki, H. Two-Orbital Model Explains the Higher Transition Temperature of the Single-Layer Hg-Cuprate Superconductor Compared to That of the La-Cuprate Superconductor. *Phys. Rev. Lett.* **2010**, *105*, 057003. [CrossRef]
21. Feiner, L.F.; Jefferson, J.H.; Raimondi, R. Effective single-band models for the high-T_c cuprates. 1. Coulomb interactions. *Phys. Rev. B* **1996**, *53*, 8751–8773. [CrossRef]
22. Bianconi, A. Lifshitz Transitions In Multi-band Hubbard Models for Topological Superconductivity in Complex Quantum Matter. *J. Supercond. Novel Magn.* **2018**, *31*, 603–610. [CrossRef]
23. Drozdov, A.P.; Eremets, M.I.; Troyan, I.A.; Ksenofontov, V.; Shylin, S.I. Conventional superconductivity at 203 Kelvin at high pressures in the sulfur hydride system. *Nature* **2015**, *525*, 73–76. [CrossRef]
24. Capitani, F.; Langerome, B.; Brubach, J.-B.; Roy, P.; Drozdov, A.; Eremets, M.I.; Nicol, E.J.; Carbotte, J.P.; Timusk, T. Spectroscopic evidence of a new energy scale for superconductivity in H_3S. *Nat. Phys.* **2017**, *13*, 859–863. [CrossRef]
25. Müller, K.A. Large, small, and especially Jahn-Teller polarons. *J. Supercond.* **1999**, *12*, 3–7. [CrossRef]
26. Keller, H.; Bussmann-Holder, A.; Müller, K.A. Jahn-Teller physics and high-T_c superconductivity. *Mat. Today* **2008**, *11*, 38–46. [CrossRef]
27. Zaanen, J.; Oleś, A.M. Carriers binding to excitons: Crystal-field excitations in doped Mott-Hubbard insulators. *Phys. Rev. B* **1993**, *48*, 7197–7215. [CrossRef]
28. Zhong, Y.; Wang, Y.; Han, S.; Lv, Y.-F.; Wang, W.-L.; Zhang, D.; Ding, H.; Zhang, Y.-M.; Wang, L.; He, K.; et al. Nodeless pairing in superconducting copper-oxide monolayer films on $Bi_2Sr_2CaCu_2O_{8+\delta}$. *Sci. Bull.* **2016**, *61*, 1239–1247. [CrossRef]
29. Jiang, K.; Wu, X.; Hu, J.; Z. Wang, Z. Nodeless High-T_c Superconductivity in the Highly Overdoped CuO_2 Monolayer. *Phys. Rev. Lett.* **2018**, *121*, 227002. [CrossRef]
30. Li, Q.; Tsay, Y.N.; Suenaga, M.; Klemm, R.A.; Gu, G.D.; Koshizuka, N. $Bi_2Sr_2CaCu_2O_{8+\delta}$ Bicrystal *c*-Axis Twist Josephson Junctions: A New Phase-Sensitive Test of Order Parameter Symmetry. *Phys. Rev. Lett.* **1999**, *83*, 4160–4163. [CrossRef]
31. Misra, S.; Oh, S.; Hornbaker, D.J.; DiLuccio, T.; Eckstein, J.N.; Yazdani, A. Atomic Scale Imaging and Spectroscopy of a CuO_2 Plane at the Surface of $Bi_2Sr_2CaCu_2O_{8+\delta}$. *Phys. Rev. Lett.* **2002**, *89*, 087002. [CrossRef]
32. Hoogenboom, B.W.; Kadowaki, K.; Revaz, B.; Fischer, Ø. Homogeneous samples of $Bi_2Sr_2CaCu_2O_{8+\delta}$. *Phys. C* **2003**, *391*, 376–380. [CrossRef]
33. Latyshev, Y.I.; Orlov, A.P.; Nikitina, A.M.; Monceau, P.; Klemm, R.A. *c*-axis transport in naturally grown $Bi_2Sr_2CaCu_2O_{8+\delta}$ cross-whisker junctions. *Phys. Rev. B* **2004**, *70*, 094517. [CrossRef]
34. Klemm, R.A. The phase-sensitive *c*-axis twist experiments on $Bi_2Sr_2CaCu_2O_{8+\delta}$ and their implications. *Philos. Mag.* **2004**, *85*, 801–853. [CrossRef]
35. Zhu, Y.; Liao, M.; Zhang, Q.; Meng, F.; Zhong, R.; Schneeloch, J.; Gu, G.; Gu, L.; Ma, X.; Zhang, D.; et al. Isotropic Josephson tunneling in c-axis twist bicrystals of $Bi_2Sr_2CaCu_2O_{8+\delta}$. *arXiv* **2019**, arXiv:1903.07965.
36. Chaloupka, J.; Khaliullin, G. Orbital Order and Possible Superconductivity in $LaNiO_3/LaMO_3$ Superlattices. *Phys. Rev. Lett.* **2008**, *100*, 016404. [CrossRef] [PubMed]
37. Knolle, J.; Eremin, I.; Moessner, R. Multiorbital spin susceptibility in a magnetically ordered state: Orbital versus excitonic spin density wave scenario. *Phys. Rev. B* **2011**, *83*, 224503. [CrossRef]

38. Veenstra, C.N.; Zhu, Z.-H.; Raichle, M.; Ludbrook, B.M.; Nicolaou, A.; Slomski, B.; Landolt, G.; Kittaka, S.; Maeno, Y.; Dil, J.H.; et al. Spin-Orbital Entanglement and the Breakdown of Singlets and Triplets in Sr_2RuO_4 Revealed by Spin- and Angle-Resolved Photoemission Spectroscopy. *Phys. Rev. Lett.* **2014**, *112*, 127002. [CrossRef]
39. Bertinshaw, J.; Kim, Y.K.; Khaliullin, G.; Kim, B.J. Square Lattice Iridates. *Annu. Rev. Condens. Matter Phys.* **2019**, *10*, 315–336. [CrossRef]
40. Varma, C.M.; Schmitt-Rink, S.; Abrahams, E. Charge transfer excitations and superconductivity in "ionic" metals. *Solid State Commun.* **1987**, *62*, 681–685. [CrossRef]
41. Emery, V.J. Theory of High-T_c Superconductivity in Oxides. *Phys. Rev. Lett.* **1987**, *58*, 2794–2797. [CrossRef]
42. Oleś, A.M.; Zaanen, J.; Fulde, P. How strongly are electrons correlated in the high-T_c superconducting materials? *Phys. B & C* **1987**, *148*, 260–263.
43. Arrigoni, E.; Aichhorn, M.; Daghofer, M.; Hanke, W. Phase diagram and single-particle spectrum of CuO_2 layers within a variational cluster approach to the 3-band Hubbard model. *New J. Phys.* **2009**, *11*, 055066. [CrossRef]
44. Hanke, W; Kiesel, M.L.; Aichhorn, M.; Brehm, S.; Arrigoni, E. The 3-band Hubbard model *versus* the 1-band model for the high-T_c cuprates: Pairing dynamics, superconductivity and the ground state phase diagram. *Eur. Phys. J. Spec. Top.* **2010**, *188*, 15–32. [CrossRef]
45. Ebrahimnejad, H.; Sawatzky, G.A.; Berciu, M. The dynamics of a doped hole in a cuprate is not controlled by spin fluctuations. *Nat. Phys.* **2014**, *10*, 951–955. [CrossRef]
46. Bianconi, A.; De Santis, M.; Flank, A.; Fontaine, A.; Lagarde, P.; Marcelli, A.; Katayamayoshida, H.; Kotani, A. Determination of the symmetry of the $3d^9L$ states by polarized Cu *L*3 XAS spectra of single crystal $YBa_2Cu_3O_{6.9}$. *Phys. C* **1988**, *153–155*, 1760–1761. [CrossRef]
47. Bianconi, A.; De Santis, M.; Di Cicco, A.; Flank, A.M.; Fontaine, A.; Lagarde, P.; Katayama-Yoshida, H.; Kotani, A.; Marcelli, A. Symmetry of the $3d^9$ ligand hole induced by doping in $YBa_2Cu_3O_{7-x}$. *Phys. Rev. B* **1988**, *38*, 7196–7199. [CrossRef]
48. Nücker, N.; Pellegrin, E.; Schweiss, P.; Fink, J.; Molodtsov, S.L.; Simmons, C.T.; Kaindl, G.; Frentrup, W.; Erb, A.; Müller-Vogt, G. Site-specific and doping-dependent electronic structure of $YBa_2Cu_3O_x$ probed by O 1*s* and Cu 2*p* x-ray-absorption spectroscopy. *Phys. Rev. B* **1995**, *51*, 8529–8542. [CrossRef]
49. Pompa, M.; Castrucci, P.; Li, C.; Udron, D.; Flank, A.M.; Lagarde, P.; Katayama-Yoshida, H.; Della Longa, S.; Bianconi, A. On the orbital angular momentum of Cu 3d hole states in superconducting $La_{2-x}Sr_xCuO_4$. *Phys. C* **1991**, *184*, 102–112. [CrossRef]
50. Chen, C.T.; Tjeng, L.H.; Kwo, J.; Kao, H.L.; Rudolf, P.; Sette, F.; Fleming, R.M. Out-of-plane orbital characters of intrinsic and doped holes in $La_{2-x}Sr_xCuO_4$. *Phys. Rev. Lett.* **1992**, *68*, 2543–2546. [CrossRef]
51. Sakakibara, H.; Suzuki, K.; Usui, H.; Kuroki, K.; Arita, R.; Scalapino, D.J.; Aoki, H. Multiorbital analysis of the effects of uniaxial and hydrostatic pressure on T_c in the single-layered cuprate superconductors. *Phys. Rev. B* **2012**, *86*, 134520. [CrossRef]
52. Seino, Y.; Kotani, A.; Bianconi, A. Effect of Rhombic Distortion on the Polarized X-Ray Absorption Spectra in High T_c Superconductors. *J. Phys. Soc. Jpn.* **1990**, *59*, 815–818. [CrossRef]
53. Bianconi, A.; Valletta, A.; Perali, A.; Saini, N.L. Superconductivity of a striped phase at the atomic limit. *Phys. C* **1998** *296*, 269–280. [CrossRef]
54. Bianconi, A.; Di Castro, D.; Bianconi, G.; Pifferi, A.; Saini, N.L.; Chou, F.C.; Johnston, D.C. ; Colapietro, M. Coexistence of stripes and superconductivity: T_c amplification in a superlattice of superconducting stripes. *Phys. C* **2000**, *341*, 1719–1722. [CrossRef]
55. Bianconi, A.; Bianconi, G.; Caprara, S.; Di Castro, D.; Oyanagi, H.; Saini, N.L. The stripe critical point for cuprates. *J. Phys. Condens. Matter* **2000**, **12**, 10655–10666. [CrossRef]
56. Bianconi, A.; Agrestini, S.; Bianconi, G.; Di Castro, D.; Saini, N.L. A quantum phase transition driven by the electron lattice interaction gives high T_c superconductivity. *J. Alloys Compd.* **2001**, **317**, 537–541. [CrossRef]
57. Bersuker, I.B. Pseudo-Jahn-Teller effect? A two-state paradigm in formation, deformation, and transformation of molecular systems and solids. *Chem. Rev.* **2013** *113*, 1351–1390. [CrossRef]
58. Müller, K.A. Recent experimental insights into HTSC materials. *Phys. C* **2000**, *341*, 11–18. [CrossRef]
59. Bussmann-Holder, A.; Keller, H.; Bishop, A.R.; Simon, A.; Micnas, R.; Müller, K.A. Unconventional isotope effects as evidence for polaron formation in cuprates. *Europhys. Lett.* **2005**, *72*, 423–429. [CrossRef]

60. Müller, K.A. The unique properties of superconductivity in cuprates. *J. Supercond. Novel Magn.* **2014**, *27*, 2163–2179. [CrossRef]
61. Zhou, J. S., Bersuker, G. I., Goodenough, J. B. Non-adiabatic electron-lattice interactions in the copper-oxide superconductors. *J. Supercond.* **1995**, *8*, 541–544. [CrossRef]
62. Bersuker, G.I.; Goodenough, J.B. Large low-symmetry polarons of the high-Tc copper oxides: formation, mobility and ordering. *Phys. C* **1997**, *274*, 267–285. [CrossRef]
63. Lanzara, A.; Zhao, G. M.; Saini, N. L.; Bianconi, A.; Conder, K.; Keller, H.; Müller, K.A. Oxygen-isotope shift of the charge-stripe ordering temperature in $La_{2-x}Sr_xCuO_4$ from x-ray absorption spectroscopy. *J. Phys. Condens. Matter* **1999**, *11*, L541–L546. [CrossRef]
64. McQueeney, R.J.; Petrov, Y.; Egami, T.; Yethiraj, M.; Shirane, G.; Endoh, Y. Anomalous Dispersion of LO Phonons in $La_{1.85}Sr_{0.15}CuO_4$ at Low Temperatures. *Phys. Rev. Lett.* **1999**, *82*, 628–631. [CrossRef]
65. Le Tacon, M.; Bosak, A.; Souliou, S.M.; Dellea, G.; Loew, T.; Heid, R.; Bohnen, K.-P.; Ghiringhelli, G.; Krisch, M.; Keimer, B. Giant phonon anomalies and central peak due to charge density wave formation in $YBa_2Cu_3O_{6.6}$. *Nat. Phys.* **2014**, *10*, 52–58. [CrossRef]
66. Miao, H.; Ishikawa, D.; Heid, R.; Le Tacon, M.; Fabbris, G.; Meyers, D.; Gu, G.D.; Baron, A.Q.R.; Dean, M.P.M. Incommensurate Phonon Anomaly and the Nature of Charge Density Waves in Cuprates. *Phys. Rev. X* **2018**, *8*, 011008. [CrossRef]
67. Weber, W. A Cu $d-d$ Excitation Model for the Pairing in the High-T_c Cuprates. *Z. Phys. B* **1988**, *70*, 323–329. [CrossRef]
68. Jarrell, M.; Krishnamurthy, H.R.; Cox, D.L. Charge-transfer mechanisms for high-T_c superconductivity. *Phys. Rev. B* **1988**, *38*, 4584–4587. [CrossRef]
69. Cox, D.L.; Jarrell, M.; Jayaprakash, C.; Krishnamurthy, H.R.; Deisz, J. Virtual Electric Quadrupole Fluctuations: A Mechanism for High T_c. *Phys. Rev. Lett.* **1989**, *62*, 2188–2191. [CrossRef]
70. Feiner, L.F.; Grilli, M.; Di Castro, C. Apical oxygen ions and the electronic structure of the high-T_c cuprates. *Phys. Rev. B* **1992**, *45*, 10647–10669. [CrossRef]
71. Buda, F.; Cox, D.L.; Jarrell, M. Random-phase-approximation analysis of orbital- and magnetic-fluctuation-mediated superconductivity in a two-band Hubbard model. *Phys. Rev. B* **1994**, *49*, 1255–1268. [CrossRef]
72. Bucci, F.; Castellani, C.; Di Castro, C.; Grilli, M. Charge fluctuations in the four-band extended Hubbard model. *Phys. Rev. B* **1995**, *52*, 6880–6893. [CrossRef]
73. Sakakibara, H.; Suzuki, K.; Usui, H.; Miyao, S.; Maruyama, I.; Kusakabe, K.; Arita, R.; Aoki, H.; Kuroki, K. Orbital mixture effect on the Fermi-surface–T_c correlation in the cuprate superconductors: Bilayer vs. single layer. *Phys. Rev. B* **2014**, *89*, 224505. [CrossRef]
74. Weber, C.; Haule, K.; Kotliar, G. Apical oxygens and correlation strength in electron- and hole-doped copper oxides. *Phys. Rev. B* **2010**, *82*, 125107. [CrossRef]
75. Zaanen, J.; Oleś, A.M. Canonical Perturbation Theory and the Two-Band Model for High-T_c Superconductors. *Phys. Rev. B* **1988**, *45*, 9423–9438. [CrossRef]
76. Zhang, F.C.; Rice, T.M. Effective Hamiltonian for the superconducting Cu Oxides. *Phys. Rev. B* **1988**, *37*, 3759–3761. [CrossRef]
77. Perkins, J.D.; Graybeal, J.M.; Kastner, M.A.; Birgeneau, R.J.; Falck, J.P.; Greven M. Mid-infrared optical absorption in undoped lamellar copper oxides. *Phys. Rev. Lett.* **1992**, *71*, 1621–1624. [CrossRef]
78. Ghiringhelli, G; Brookes, N.B.; Annese, E.; Berger, H.; Dallera, C.; Grioni, M.; Perfetti, L.; Tagliaferri, A.; Braicovich, L. Low Energy Electronic Excitations in the Layered Cuprates Studied by Copper L_3 Resonant Inelastic X-Ray Scattering. *Phys. Rev. Lett.* **2004**, *92*, 117406. [CrossRef]
79. Lorenzana, J.; Sawatzky, G.A. Phonon assisted multimagnon optical absorption and long lived two-magnon states in undoped lamellar copper oxides. *Phys. Rev. Lett.* **1995**, *74*, 1867–1870. [CrossRef]
80. Ament, L.J.P.; van Veenendaal, M.; Devereaux, T.P.; Hil, J.P.; van den Brink, J. Resonant inelastic x-ray scattering studies of elementary excitations. *Rev. Mod. Phys.* **2011**, *83*, 705–767. [CrossRef]
81. Hozoi, L.; Siurakshina, L.; Fulde, P.; van den Brink, J. *Ab Initio* determination of Cu 3*d* orbital energies in layered copper oxides. *Sci. Rep.* **2011**, *1*, 65. [CrossRef] [PubMed]
82. Moretti Sala, M.; Bisogni, V.; Aruta, C.; Balestrino, G.; Berger, H.; Brookes, N.B.; de Luca, G.M.; Di Castro, D.; Grioni, M.; Guarise, M.; et al. Energy and symmetry of *dd* excitations in undoped layered cuprates measured by Cu L_3 resonant inelastic x-ray scattering. *New J. Phys.* **2011**, *13*, 043026. [CrossRef]

83. Bianconi, A.; Castrucci, P.; Fabrizi, A.; Pompa, M.; Flank, A.M.; Lagarde, P.; Katayama-Yoshida, H.; Calestani, G. Correlation between mixing of Cu *d* orbitals and Tc determined by polarized Cu L_3 XAS: Experimental evidence for pairing mediated by *d-d* excitations. *Phys. C* **1989**, *162*, 209–210. [CrossRef]
84. Nücker, N.; Romberg, H.; Xi, X.X.; Fink, J.; Gegenheimer, B.; Zhao, Z.X. Symmetry of holes in high-T_c superconductors. *Phys. Rev. B* **1989**, *39*, 6619–6629. [CrossRef]
85. Khomskii, D.I.; Neimark, E.I. Orbital structure of copper in high temperature superconductors. *Phys. C* **1991**, *173*, 342–346. [CrossRef]
86. Ellis, D.S.; Huang, Y.B.; Olalde-Velasco, P.; Dantz, M.; Pelliciari, J.; Drachuck, G.; Ofer, R.; Bazalitsky, G.; Berger, J.; Schmitt, T.; et al. Correlation of the superconducting critical temperature with spin and orbital excitations in $(Ca_xLa_{1-x})(Ba_{1.75-x}La_{0.25+x})Cu_3O_y$ as measured by resonant inelastic x-ray scattering. *Phys. Rev. B* **2015**, *92*, 104507. [CrossRef]
87. Fumagalli, R.; Braicovich, L.; Minola, M.; Peng, Y.Y.; Kummer, K.; Betto, D.; Rossi, M.; Lefrancois, E.; Morawe, C; Salluzzo, M. Polarization resolved Cu L_3-edge resonant inelastic x-ray scattering of orbital and spin excitations in $NdBa_2Cu_3O_{7-\delta}$. *arXiv* **2019**, arXiv:1902.05471.
88. Kang, M.; Pelliciari, J.; Krockenberger, Y.; Li, J.; McNally, D.E.; Paris, E.; Liang, R.; Hardy, W.N.; Bonn, D.A.; Yamamoto, H.; et al. Resolving the nature of electronic excitations in resonant inelastic x-ray scattering. *Phys. Rev. B* **2019**, *99*, 045105. [CrossRef]
89. Kugel, K.I.; Khomskii, D.I. Jahn-Teller Effect and Magnetism: Transition Metal Compounds. *Usp. Fiz. Nauk* **1982**, *25*, 621–664. [CrossRef]
90. Feiner, L.F.; Oleś, A.M.; Zaanen, J. Quantum Melting of Magnetic Order due to Orbital Fluctuations. *Phys. Rev. Lett.* **1997**, *78*, 2799–2802. [CrossRef]
91. Tokura, Y.; Nagaosa, N. Orbital Physics in Transition-Metal Oxides. *Science* **2000**, *288*, 462–468. [CrossRef]
92. Oleś, A.M.; Khaliullin, G.; Horsch, P.; Feiner, L.F. Fingerprints of spin-orbital physics in cubic Mott insulators: Magnetic exchange interactions and optical spectral weights. *Phys. Rev. B* **2005**, *72*, 214431. [CrossRef]
93. Khaliullin, G. Orbital Order and Fluctuations in Mott Insulators. *Prog. Theor. Phys. Suppl.* **2005**, *160*, 155–202. [CrossRef]
94. Normand, B.; Oleś, A.M. Frustration and entanglement in the t_{2g} spin-orbital model on a triangular lattice: Valence-bond and generalized liquid states. *Phys. Rev. B* **2008**, *78*, 094427. [CrossRef]
95. Corboz, P.; Lajkó, M.; Laüchli, A.M.; Penc, K.; Mila, F. Spin-Orbital Quantum Liquid on the Honeycomb Lattice. *Phys. Rev. X* **2012**, *2*, 041013. [CrossRef]
96. Oleś, A.M. Fingerprints of Spin-Orbital Entanglement in Transition Metal Oxides. *J. Phys. Condens. Matter* **2012**, *24*, 313201. [CrossRef] [PubMed]
97. Schlappa, J.; Wohlfeld, K.; Zhou, K.J.; Mourigal, M.; Haverkort, M.W.; Strocov, V.N.; Hozoi, L.; Monney, C.; Nishimoto, S.; Singh, S.; et al. Spin-orbital separation in the quasi-one-dimensional Mott insulator Sr_2CuO_3. *Nature* **2012**, *485*, 82–85. [CrossRef] [PubMed]
98. Bisogni, V.; Wohlfeld, K.; Nishimoto, S.; Monney, C.; Trinckauf, J.; Zhou, K.; Kraus, R.; Koepernik, K.; Sekar, C.; Strocov, V.; et al. Orbital Control of Effective Dimensionality: From Spin-Orbital Fractionalization to Confinement in the Anisotropic Ladder System $CaCu_2O_3$. *Phys. Rev. Lett.* **2015**, *114*, 096402. [CrossRef]
99. Wohlfeld, K.; Daghofer, M.; Nishimoto, S.; Khaliullin, G.; van den Brink, J. Intrinsic Coupling of Orbital Excitations to Spin Fluctuations in Mott Insulators. *Phys. Rev. Lett.* **2011**, *107*, 247201. [CrossRef]
100. Wohlfeld, K.; Nishimoto, S.; Haverkort, M.W.; van den Brink, J. Microscopic origin of spin-orbital separation in Sr_2CuO_3. *Phys. Rev. B* **2013**, *88*, 195138. [CrossRef]
101. Brzezicki, W.; Oleś, A.M.; Cuoco, M. Spin-Orbital Order Modified by Orbital Dilution in Transition-Metal Oxides: From Spin Defects to Frustrated Spins Polarizing Host Orbitals. *Phys. Rev. X* **2015**, *5*, 011037. [CrossRef]
102. Brzezicki, W. Spin, orbital and topological order in models of strongly correlated electrons. *arXiv* **2019**, arXiv:1904.11772.
103. Comin, R.; Damascelli, A. Resonant X-Ray Scattering Studies of Charge Order in Cuprates. *Annu. Rev. Condens. Matter Phys.* **2016**, *7*, 369–405. [CrossRef]
104. Liu, Q.Q.; Yang, H.; Qin, X.M.; Yu, Y.; Yang, L.X.; Li, F.Y.; Yu, R.C.; Jin, C.Q.; Uchida, S. Enhancement of the superconducting critical temperature of $Sr_2CuO_{3+\delta}$ up to 95K by ordering dopant atoms. *Phys. Rev. B* **2006**, *74*, 100506(R). [CrossRef]

105. Maier, T.A.; Berlijn, T.; Scalapino, D.J. d-wave and $s^{\pm}$ Pairing Strengths in $Ba_2CuO_{3+\delta}$. *arXiv* **2018**, arXiv:1809.04156.
106. Geballe, T.H.; Marezio, M. Enhanced superconductivity in Sr_2CuO_{4-v}. *Phys. C* **2009**, *469*, 680–684. [CrossRef]
107. Li, W.M.; Cao, L.P.; Zhao, J.F.; Yu, R.Z.; Zhang, J.; Liu, Y.; Liu, Q.Q.; Zhao, G.Q.; Wang, X.C.; Hu, Z.; et al. A new superconductor of cuprates with unique features. *arXiv* **2018**, arXiv:1808.09425.
108. Uchida, M.; Ishizaka, K.; Hansmann, P.; Yang, X.; Sakano, M.; Miyawaki, J.; Arita, R.; Kaneko, Y.; Takata, Y.; Oura, M.; et al. Orbital characters of three-dimensional Fermi surfaces in $Eu_{2-x}Sr_xNiO_4$ as probed by soft-x-ray angle-resolved photoemission spectroscopy. *Phys. Rev. B* **2011**, *84*, 241109(R). [CrossRef]
109. Hansmann, P.; Yang, X.; Toschi, A.; Khaliullin, G.; Andersen, O.K.; Held K. Turning a Nickelate Fermi Surface into a Cupratelike One through Heterostructuring. *Phys. Rev. Lett.* **2009**, *103*, 016401. [CrossRef] [PubMed]
110. Disa, A.S.; Kumah, D.P.; Malashevich, A.; Chen, H.; Arena, D.A.; Specht, E.D.; Ismail-Beigi, S.; Walker, F.J.; Ahn, C.H. Orbital Engineering in Symmetry-Breaking Polar Heterostructures. *Phys. Rev. Lett.* **2015**, *114*, 026801. [CrossRef] [PubMed]
111. Wu, M.; Benckiser, E.; Haverkort, M.V.; Frano, A.; Lu, Y.; Nwanko, N.; Brück, S.; Audehm, P.; Goering, E.; Mache, S.; et al. Strain and composition dependence of the orbital polarization in nickelate superlattices. *Phys. Rev. B* **2013**, *88*, 125124. [CrossRef]
112. Hepting, M.; Minola, M.; Frano, A.; Cristiani, G.; Logvenov, G.; Schierle, E.; Wu, M.; Bluschke, M.; Weschke, E.; H.-U. Habermeier, H.-U.; et al. Tunable spin and charge order. *Phys. Rev. Lett.* **2014**, *113*, 227206. [CrossRef]
113. Zhang, J.; Botana, A.S.; Freeland, J.W.; Phelan, D.; Zheng, H.; Pardo, V.; Norman, M.R.; Mitchell, J.F. Large orbital polarization in a metallic square-planar nickelate. *Nat. Phys.* **2017**, *13*, 864–869. [CrossRef]
114. Botana, A.S.; Pardo, V.; Norman, M.R. Electron doped layered nickelates: Spanning the phase diagram of the cuprates. *Phys. Rev. Mater.* **2017**, *1*, 021801(R). [CrossRef]
115. Le, C.; Zeng, J.; Gu, Y.; Cao, G.-H.; Hub, J. A possible family of Ni-based high temperature superconductors. *Sci. Bull.* **2018**, *63*, 957–963. [CrossRef]
116. Lu, F.; Wang, W.-H.; Xie, X.; Zhang, F.-C. Correlation effects in the electronic structure of the Ni-based superconducting KNi_2S_2. *Phys. Rev. B* **2013**, *87*, 115131. [CrossRef]
117. Maeno, Y.; Hashimoto, H.; Yoshida, K.; Nishizaki, S.; Fujita, T.; Bednorz, J.G.; Lichtenberg, F. Superconductivity in a layered perovskite without copper. *Nature* **1994**, *372*, 532–534. [CrossRef]
118. Agterberg, D.F.; Rice, T.M.; Sigrist, M. Orbital Dependent Superconductivity in Sr_2RuO_4. *Phys. Rev. Lett.* **1997**, *78*, 3374–3377. [CrossRef]
119. Maeno, Y.; Rice, T.M.; Sigrist, M. The Intriguing Superconductivity of Strontium Ruthenate. *Phys. Today* **2001**, *54*, 42–47. [CrossRef]
120. Suderow, H.; Crespo, V.; Guillamon, I.; Vieira, S.; Servant, S.; Leyey, P.; Brison, J.P.; Floquet, J. A nodeless superconducting gap in Sr_2RuO_4 from tunneling spectroscopy. *New J. Phys.* **2009**, *11*, 093004. [CrossRef]
121. Pustogow, A.; Luo, Yonkang; Chronister, A.; Su, Y.-S.; Sokolov, D.A.; Jerzembeck, F.; Mackenzie, A.P.; Hicks, C.W.; Kikugawa, N.; Raghu, S.; et al. Pronounced drop of ^{17}O NMR Knight shift in superconducting state of Sr_2RuO_4. *arXiv* **2019**, arXiv:1904.00047.
122. Wang, Q.H.; Platt, C.; Yang, Y.; Honerkamp, C.; Zhang, F.C.; Hanke, W.; Rice, T.M.; Thomale, R. Theory of superconductivity in a three-orbital model of Sr_2RuO_4. *Europhys. Lett.* **2013**, *104*, 17013. [CrossRef]
123. Imai, Y.; Wakabayashi, K.; Sigrist, M. Topological and edge state properties of a three-band model for Sr_2RuO_4. *Phys. Rev. B* **2013**, *88*, 144503. [CrossRef]
124. Akebi, S; Kondo, T.; Nakayama, M.; Kuroda, K.; Kunisada, So; Taniguchi, H.; Maeno, Y.; Shin, S. Low-energy electron-mode couplings in the surface bands of Sr_2RuO_4 revealed by laser-based angle-resolved photoemission spectroscopy. *Phys. Rev. B* **2019**, *99*, 081108(R). [CrossRef]
125. Khaliullin, G.; Koshibae, W.; Maekawa, S. Low Energy Electronic States and Triplet Pairing in Layered Cobaltate. *Phys. Rev. Lett.* **2004**, *93*, 176401. [CrossRef]
126. Jackeli, G.; Khaliullin, G. Mott Insulators in the Strong Spin-Orbit Coupling Limit: From Heisenberg to a Quantum Compass and Kitaev Models. *Phys. Rev. Lett.* **2009**, *102*, 017205. [CrossRef] [PubMed]
127. Kim, B.J.; Jin, H.; Moon, S.J.; Kim, J.-Y.; Park, B.G.; Leem, C.S.; Yu, J.; Noh, T.W.; Kim, C.; Oh, S.-J.; et al. Novel $J_{\mathrm{eff}} = 1/2$ Mott State Induced by Relativistic Spin-Orbit Coupling in Sr_2IrO_4. *Phys. Rev. Lett.* **2008**, *101*, 076402. [CrossRef]
128. Kim, B.J.; Ohsumi, H.; Komesu, T.; Sakai, S.; Morita, T.; Takagi, H.; Arima, T. Phase-Sensitive Observation of a Spin-Orbital Mott State in Sr_2IrO_4. *Science* **2009**, *323*, 1329–1332. [CrossRef]

129. Kim, J.; Casa, D.; Upton, M.H.; Gog, T.; Kim, Y.-J.; Mitchell, J.F.; van Veenendaal, M.; Daghofer, M.; van den Brink, J.; Khaliullin, G.; et al. Magnetic Excitation Spectra of Sr_2IrO_4 Probed by Resonant Inelastic X-Ray Scattering: Establishing Links to Cuprate Superconductors. *Phys. Rev. Lett.* **2012**, *108*, 177003. [CrossRef]
130. Liu, H.; Khaliullin, G. Pseudo-Jahn-Teller Effect and Magnetoelastic Coupling in Spin-Orbit Mott Insulators. *Phys. Rev. Lett.* **2019**, *122*, 057203. [CrossRef]
131. Kim, Y.K.; Krupin, O.; Denlinger, J.D.; Bostwick, A.; Rotenberg, E.; Zhao, Q.; Mitchell, J.F.; Allen, J.W.; Kim, B.J. Fermi arcs in a doped pseudospin-1/2 Heisenberg antiferromagnet. *Science* **2014**, *160*, 1329–1332. [CrossRef]
132. Imada, M. Universality classes of metal-insulator transitions in strongly correlated electron systems and mechanism of high-temperature superconductivity. *Phys. Rev. B* **2005**, *72*, 075113. [CrossRef]
133. Andersen, O.K.; Boeri, L. On the multi-orbital band structure and itinerant magnetism of iron-based superconductors. *Ann. Phys.* **2011**, *523*, 8–50. [CrossRef]
134. Ferber, J.; Jeschke, H.O.; Valentí, R. Fermi Surface Topology of LaFePO and LiFeP. *Phys. Rev. Lett.* **2012**, *109*, 236403. [CrossRef] [PubMed]
135. Raghu, S.; Qi, X.L.; Liu, C.X.; Scalapino, D.J.; Zhang, S.C. Minimal two-band model of the superconducting iron oxypnictides. *Phys. Rev. B* **2013**, *88*, 144503. [CrossRef]
136. Daghofer, M.; Nicholson, A.; Moreo, A.; Dagotto, E. Three orbital model for the iron-based superconductors. *Phys. Rev. B* **2010**, *81*, 014511. [CrossRef]
137. Fernandes, R.M.; Schmalian, J. Competing order and nature of the pairing state in the iron pnictides. *Phys. Rev. B* **2010**, *82*, 014521. [CrossRef]
138. Nicholson, A.; Ge, W.; Zhang, X.; Riera, J.; Daghofer, M.; Oleś, A.M.; Martins, G.B.; Moreo, A.; Dagotto, E. Competing Pairing Symmetries in a Generalized Two-Orbital Model for the Pnictide Superconductors. *Phys. Rev. Lett.* **2011**, *106*, 217002. [CrossRef]
139. Nicholson, A.; Ge, W.; Riera, J.; Daghofer, M.; Moreo, A.; Dagotto, E. Pairing symmetries of a hole-doped extended two-orbital model for the pnictides. *Phys. Rev. B* **2012**, *85*, 024532. [CrossRef]
140. Ptok, A.; Kapcia, K.J.; Cichy, A.; Oleś, A.M.; Piekarz, P. Magnetic Lifshitz transition and its consequences in multi-band iron-based superconductors. *Sci. Rep.* **2017**, *7*, 41979. [CrossRef] [PubMed]
141. Tafti, F.F.; Juneau-Fecteau, A.; Delage, M.E.; René de Cotret, S.; Reid, J.P.; Wang, A.F.; Luo, X.G.; Chen, X.H.; Doiron-Leyraud, N.; Taillefer, L. Sudden reversal in the pressure dependence of T_c in the iron-based superconductor KFe_2As_2. *Nat. Phys.* **2013**, *9*, 349–352. [CrossRef]
142. Qi, Q.; Abrahams, E. Strong Correlations and Magnetic Frustration in the High T_c Iron Pnictides. *Phys. Rev. Lett.* **2008**, *101*, 076401.
143. Krüger, F.; Kumar, S.; Zaanen, J.; van den Brink, J. Spin-orbital frustrations and anomalous metallic state in iron-pnictide superconductors. *Phys. Rev. B* **2009**, *79*, 054504. [CrossRef]
144. Fink, J.; Rienks, E.D.L.; Thirupathaiah, S.; Nayak, J.; van Roekeghem, A.; Biermann, S.; Wolf, T.; Adelmann, P.; Jeevan, H.S.; Gegenwart, P.; et al. Experimental evidence for importance of Hund's exchange interaction for incoherence of charge carriers in iron-based superconductors. *Phys. Rev. B* **2017**, *95*, 144513. [CrossRef]
145. Yaresko, A.N.; Liu, G.-Q.; Antonov, V.N.; Andersen, O.K. Interplay between magnetic properties and Fermi surface nesting in iron pnictides. *Phys. Rev. B* **2009**, *79*, 144421. [CrossRef]
146. Wysocki, A.L.; Belashchenko, K.D.; Antropov, V.P. Consistent model of magnetism in ferropnictides. *Nat. Phys.* **2011**, *7*, 485–489. [CrossRef]
147. Yu, R.; Wang, Z.; Goswami, P.; Nievidomskyy, A.H.; Si, Q.; Abrahams, E. Spin dynamics of a J_1-J_2-K model for the paramagnetic phase of iron pnictides. *Phys. Rev. B* **2012**, *86*, 085148. [CrossRef]
148. Glasbrenner, J.K.; Mazin, I.I.; Jeschke, H.O.; Hirschfeld, P.J.; Valentí, R. Effect of magnetic frustration on nematicity and superconductivity in Fe chalcogenides. *Nat. Phys.* **2015**, *11*, 953–958. [CrossRef]
149. Chaloupka, J.; Khaliullin, G. Spin-State Crossover Model for the Magnetism of Iron Pnictides. *Phys. Rev. Lett.* **2013**, *110*, 207205. [CrossRef]
150. Dai, P.C.; Hu, J.P.; Dagotto, E. Magnetism and its microscopic origin in iron-based high-temperature superconductors. *Nat. Phys.* **2012**, *8*, 709–718. [CrossRef]
151. Beak, S.-H.; Efremov, D.V.; Ok, J.M.; Kim, J.S.; van den Brink, J.; Büchner, B. Orbital-driven nematicity in FeSe. *Nat. Mat.* **2014**, *14*, 210–214. [CrossRef]

152. Watson, M.D.; Kim, T.K.; Haghighirad, A.A.; Davies, N.R.; McCollam, A.; Narayanan, A.; Blake, S.F.; Chen, Y.L.; Ghannadzadeh, S.; Schofield, A.J.; et al. Emergence of nematic electronic state in FeSe. *Phys. Rev. B* **2015**, *91*, 155106. [CrossRef]
153. Fernandes, R.M.; Chubukov, A.V.; Knolle, J.; Eremin, I.; Schmalian, J. Preemptive nematic order, pseudogap, and orbital order in the iron pnictides. *Phys. Rev. B* **2012**, *85*, 024534. [CrossRef]
154. Kontani, H.; Onari, S. Orbital-Fluctuation-Mediated Superconductivity in Iron Pnictides: Analysis of the Five-Orbital Hubbard-Holstein Model. *Phys. Rev. Lett.* **2010**, *104*, 157001. [CrossRef] [PubMed]
155. Onari, S.; Kontani, H. Self-consistent Vertex Correction Analysis for Iron-based Superconductors: Mechanism of Coulomb Interaction-Driven Orbital Fluctuations. *Phys. Rev. Lett.* **2012**, *109*, 137001. [CrossRef]
156. Saito, T.; Onari, S.; Kontani H. Orbital fluctuation theory in iron pnictides: Effects of As-Fe-As bond angle, isotope substitution, and Z^2-orbital pocket on superconductivity. *Phys. Rev. B* **2010**, *82*, 144510. [CrossRef]
157. Chubukov, A.V.; Khodas, M.; Fernandes, R.M. Magnetism, Superconductivity, and Spontaneous Orbital Order in Iron-Based Superconductors: Which Comes First and Why? *Phys. Rev. X* **2016**, *6*, 041045. [CrossRef]
158. Liu, D.F.; Li, C.; Huang, J.W.; Lei, B.; Wang, L.; Wu, X.X.; Shen, B.; Gao, Q.; Zhang, Y.X.; Liu, X.; et al. Orbital Origin of Extremely Anisotropic Superconducting Gap in Nematic Phase of FeSe Superconductor. *Phys. Rev. X* **2018**, *8*, 031033. [CrossRef]
159. Hashimoto, H.; Ota, Y.; Yamamoto, H.Q.; Suzuki, Y.; Shimojima, T.; Watanabe, S.; Chen, C.; Kashara, S.; Matsuda, Y.; Shibauchi, T.; et al. Superconducting gap anisotropy sensitive to nematic domains in FeSe. *Nat. Commun.* **2018**, *9*, 282. [CrossRef]
160. Sprau, P.O.; Kostin, A.; Kreisel, A.; Böhmer, A.E.; Taufour, V.; Canfield, P.C.; Mukherjee, S.; Hirschfeld, P.J.; Andersen, B.M.; Séamus Davis, J.C. Discovery of orbital-selective Cooper pairing in FeSe. *Science* **2017**, *357*, 75–80. [CrossRef]
161. Nica, E.M.; Yu, R.; Si, Q. Orbital-selective pairing and superconductivity in iron selenides. *NPJ Quantum Mater.* **2017**, *2*, 24. [CrossRef]
162. Ptok, A.; Kapcia, K.J.; Piekarz, P.; Oleś, A.M. The *ab initio* study of unconventional superconductivity in $CeCoIn_5$ and FeSe. *New J. Phys.* **2017**, *19*, 063039. [CrossRef]
163. Li, Y.; Yin, Z.; Wang, X.; Tam, D.W.; Abernathy, D.L.; Podlesnyak, A.; Zhang, C.; Wang, M.; Xing, L.; Jin, C.; et al. Orbital Selective Spin Excitations and their Impact on Superconductivity of $LiFe_{1-x}Co_xAs$. *Phys. Rev. Lett.* **2016**, *116*, 247001. [CrossRef]
164. Gawraczyński, J.; Kurzydłowski, D.; Ewings, R.A.; Bandaru, S.; Mazej, Z.; Ruani, G.; Bergenti, I.; Jaroń, T.; Ozarowski, A.; Hill, S.; et al. Silver route to cuprate analogs. *PNAS* **2019**, *116*, 1812857. [CrossRef]
165. Jarlborg, T.; Bianconi, A. Multiple Electronic Components and Lifshitz Transitions by Oxygen Wires Formation in Layered Cuprates and Nickelates. *Condens. Matter* **2019**, *4*, 15. [CrossRef]